Antiviral Research 170 (2019) 104529

Contents lists available at ScienceDirect

Antiviral Research

journal homepage: www.elsevier.com/locate/antiviral

T-705 induces lethal mutagenesis in Ebola and Marburg populations in macaques

Nicole Espy, Elyse Nagle, Brad Pfeffer, Karla Garcia, Alex J. Chitty, Michael Wiley, Mariano Sanchez-Lockhart, Sina Bavari, Travis Warren, Gustavo Palacios*

United States Army Medical Research Institute of Infectious Diseases, Fort Detrick, Maryland, USA

A B S T R A C T

Nucleoside analogues (NA) disrupt RNA viral RNA-dependent RNA polymerase (RdRP) function and fidelity for multiple viral families. The mechanism of action (MOA) of T-705 has been attributed alternatively or concurrently to chain termination and lethal mutagenesis depending on the viral species during *in vitro* studies. In this study, we evaluated the effect of T-705 on the viral population in non-human primates (NHPs) after challenge with Ebola virus (EBOV) or Marburg virus (MARV) to identify the predominant *in vivo* MOA. We used common virological assays in conjunction with deep sequencing to characterize T-705 effects. T-705 exhibited antiviral activity that was associated with a reduction in specific infectivity and an accumulation of low frequency nucleotide variants in plasma samples collected day 7 post infection. Stranded analysis of deep sequencing data to identify chain termination demonstrated no change in the transcriptional gradient in negative stranded viral reads and minimal changes in positive stranded viral reads in T-705 treated animals, questioning as a MOA *in vivo*. These findings indicate that lethal mutagenesis is a MOA of T-705 that may serve as an indication of therapeutic activity of NAs for evaluation in clinical settings. This study expands our understanding of MOAs of these compounds for the Filovirus family and provides further evidence that lethal mutagenesis could be a preponderant MOA for this class of therapeutic compounds.

1. Introduction

Ebola virus (EBOV) and Marburg virus (MARV) are single-stranded, non-segmented negative-sense RNA virus in the *Filoviridae* family that induce severe and often fatal hemorrhagic disease in primates (Kuhn, 2008). Filoviruses contain a ~19 kb genome that encodes seven viral genes whose expression is mediated by the Large or RNA-dependent RNA polymerase (L or RdRP). After viral entry, the RdRP transcribes these viral genes in the cytoplasm into individual mRNAs such that there is a decreasing gradient in transcript levels (Sanchez et al., 1993; Shabman et al., 2014). During viral assembly, the EBOV or MARV RdRP copies the viral genome into positive-sense anti-genomes that serve as templates for new progeny genomes. The EBOV and MARV RdRPs are characterized by a high mutation rate (Andino and Domingo, 2015; Drake and Holland, 1999; Sanjuan et al., 2010). The rate of interhost mutation of EBOV observed during the 2014 Ebola outbreak was $9{\cdot}10^{-4}$ mutations/base/genome (Kugelman et al., 2015b); the intrahost mutation rate during acute and persistent infection is $9.63{\cdot}10^{-4}$ and $8.95{\cdot}10^{-4}$ mutations/base/genome, respectively (Whitmer et al., 2018). The low fidelity of RdRP provides an opportunity to develop antiviral compounds to further destabilize and inhibit viral replication (Baranovich et al., 2013).

Nucleoside analogues (NAs) are a class of compounds that have demonstrated antiviral activity on RNA viruses, including EBOV. NAs structurally mimic natural nucleotides competing with them for incorporation by the viral RdRP in the nascent RNA. The mechanism of action (MOA) of NAs vary per compound structure and the virus acted upon. Chain termination, in which the compound stalls the RdRP and terminates RNA elongation, results in truncated viral genomes (Arts and Wainberg, 1994, 1996). Lethal mutagenesis has been described as an alternative MOA, in which the compound disrupts the fidelity of the RdRP, leading to base mismatches and further loss of fitness without resulting in the generation of truncated genomes (Crotty and Andino, 2002). Interestingly, the base mismatches generated by lethal mutagenesis leave a footprint of mutations in the viral RNA that is characteristic of the NA used (Crotty et al., 2001).

Favipiravir, or T-705, is a nucleobase that could act as a guanosine or adenosine analogue (Jin et al., 2013). T-705 has shown antiviral activity against EBOV and resulted in delayed time to death in infected rodents and in primates (Bixler et al., 2017; Guedj et al., 2018; Oestereich et al., 2014; Smither et al., 2014). Although T-705 has been tested in human cases during the 2014 Western African outbreak with disappointing results (Nguyen et al., 2017; Sissoko et al., 2016), it has been suggested that the human T-705 therapeutic dose was not reached with the dosing schedule selected (Nguyen et al., 2017; Oestereich et al., 2014; Sissoko et al., 2016). The main MOA for T-705 has been

* Corresponding author.
E-mail address: gustavo.f.palacios.civ@mail.mil (G. Palacios).

https://doi.org/10.1016/j.antiviral.2019.06.001
Received 30 May 2019; Accepted 2 June 2019
Available online 10 June 2019

attributed to be both chain termination and lethal mutagenesis for the RNA viruses Influenza A, Hepatitis C, and norovirus *in vitro* (Arias et al., 2014; Baranovich et al., 2013; de Avila et al., 2016; Fung et al., 2014; Jin et al., 2013). Contrarily, lethal mutagenesis was not an important contributor to *in vitro* antiviral activity on Chikungunya (Delang et al., 2014). Very few studies have investigated the MOA of T-705 *in vivo,* as has been done for ribavirin (Arias et al., 2014; Asahina et al., 2005; Dietz et al., 2013; Guedj et al., 2018). Recently, Guedj and colleagues presented findings indicating that treatment of EBOV-infected non-human primates with T-705 induces survivorship and an increase in mutagenesis in EBOV viral population (Guedj et al., 2018).

Here, we perform an *a posteriori* virologic and genomic analyses of plasma collected during a previously published study that evaluated the capability of T-705 to increase NHP survivorship against a lethal challenge of EBOV and MARV (Bixler et al., 2017) to discern the *in vivo* MOA of T-705. We used deep sequencing to confirm that T-705 treatment is associated with increased mutagenesis on EBOV and MARV genomes, a decrease in EBOV specific infectivity, and an indeterminate effect of chain termination restricted to positively stranded RNA. These data indicate that T-705 has a dual MOA against filoviruses *in vivo*.

2. Materials and methods

2.1. Viruses

Ebola Kikwit (EBOV-Kik) and Marburg Angola (MARV-Ang) viruses were prepared at United States Army Research Institute for Infectious Diseases (Bixler et al., 2017; Kugelman et al., 2012, 2016).

2.2. Compounds

T-705 was synthesized by Toyama Chemical Co. and provided by MediVector, Inc.

2.3. Animal studies

The NHP experimental design, dosing, and clinical evaluation has been described previously (Bixler et al., 2017). Briefly, healthy cynomolgus macaques (*Macaca fascicularis*) were challenged with an intramuscular injection of a target dose of 1000 plaque forming units (PFU) of EBOV-Kik or MARV-Ang. NHP infected with EBOV-Kik were randomly assigned into vehicle or compound treated groups. NHP were administered either a 0.4% carboxymethylcellulose in water vehicle or 250 mg kg^{-1} T-705 orally twice on day 0 post infection (poi), and 150 mg kg^{-1} T-705 twice daily from day 1 to day 13 poi. NHP infected with MARV-Ang were randomly assigned into vehicle or compound treated groups, for which 4 macaques were intravenously administered 7.46% meglumine in water and 6 macaques were intravenously administered 250 mg kg^{-1} T-705 in vehicle twice daily on day 0 poi, and 150 mg kg^{-1} T-705 twice daily from day 1 to day 13 poi. Study personnel responsible for assessing animal health and administering treatments were experimentally blinded to group assignment of animals. The primary endpoint of each study was survivorship. Animal research at U.S. Army Medical Research Institute of Infectious Diseases (USAMRIID) was conducted under an Institutional Animal Care and Use Committee (IACUC) approved protocol in compliance with the Animal Welfare Act, PHS Policy, and other federal statutes and regulations relating to animals and experiments involving animals (2011). Survival contingency tables were plotted using GraphPad Prism version 7.03 for Windows (La Jolla, CA).

2.4. Virologic assays

Quantitative measurement of viral RNA copies by EBOV Quantitative RT-PCR (qRT-PCR) and viral titers by EBOV plaque assays has been described elsewhere (Bixler et al., 2017; Warren et al., 2016). qRT-PCR quantitation measurement against standard curves were generated by synthetic RNA provided RNA copies per reaction per mL plasma. The lower limits of quantification for EBOV and MARV-Ang were 8.0×10^4 and 8.0×10^5 copies per mL, respectively. The lower limit of quantification of the EBOV plaque assays were 1000 PFU/mL. MARV-Ang samples were not available to perform plaque assays.

Unpaired two-tailed *t* tests between treatment group values for qRT-PCR, plaque, and specific infectivity data were performed using GraphPad Prism version 7.03 for Windows (La Jolla, CA).

2.5. Genomic sequencing

Plasma samples collected from NHPs were deactivated in Trizol LS 1:3. RNA was extracted from samples with quantifiable qRT-PCR viral titers using the PureLink RNA Mini Kit (Invitrogen, Carlsbad, CA). cDNA libraries of the viral genomes were generated using the TruSeq RNA Access Library Kit according to manufacturer's protocol (Illumina, San Diego, CA). In summary, total RNA was enzymatically fragmented and first strand cDNA synthesis was initiated with random hexamers. Second strand synthesis removed the RNA template and incorporates dUTP, which prevents second strand amplification during sequencing, to preserve information on the strandedness of the input RNA (Borodina et al., 2011). The double stranded cDNA was cleaned and ligated to dual-indexed Nextera adaptors. The resulting cDNA libraries were PCR amplified using primers mapped to the adaptors and quality controlled for proper concentration and product size using the Agilent 2200 Tapestation (Agilent, Santa Clara, CA), and the KAPA qPCR kit (Kapa Biosystems, Woburn, MA). EBOV specific sequences were extracted and purified from the total cDNA library through a two-step hybridization protocol using filovirus specific 80mer biotinylated oligos that map to the reference genome (Illumina, San Diego, CA). EBOV libraries were pooled to equimolar volumes and cluster amplified on the Illumina cBot. Libraries were sequenced on the Illumina HiSeq 2500 using a 101bp paired-end format. MARV-Ang libraries were pooled to equimolar volumes and sequenced on an Illumina MiSeq using a 101bp paired-end format.

Dual-indexed, paired ended FASTQs were processed and analyzed by the in-house VSALIGN software program (Espy et al., 2018; Kugelman et al., 2015a, 2017). In short, VSALIGN was designed to clean, align and analyze deep sequencing data. Analyses included subclonal diversity estimates and indel, transition, transversion frequencies in each sample, as well as single nucleotide variants (SNV) frequencies at each position in the genome. To do so, samples were cleaned by selecting reads with quality score above Q30, removing chimeras and duplicate reads, and filtering out primer sequences and low complexity reads. Sequences were aligned to the reference sequence (Zaire ebola virus isolate Ebola virus/H. sap-tc/COD/1995/Kikwit-9510621 clone R4415; GenBank accession number KT762962 or Lake Victoria Marburgvirus/H. sap-wt/AGO/2005/Ang1386; DQ447655) using DNASTar Lasergene nGen (Madison, WI) and MOSAIK (Lee et al., 2014. The EBOV-Kik reference sequence varies from the challenge stock used in this study as described previously (Kugelman et al., 2012). SNVs and indels were called for positions with a target depth of 200 reads to limit efficiency biases.

Alignment files for all the libraries assessed here are available at Bioproject PRJNA483443 and National Center for Biotechnology Information Sequence Read Archive project number SRP155828.

The sequence depth of each position in the filoviral genomes were derived using SAMtools version 1.9 (Li et al., 2009).

Results were plotted using GraphPad Prism version 7.03 for Windows (La Jolla, CA).

Table 1
Study information.

Challenge Virus	Group	Number of Animals (sex)	Treatment Dose	Treatment Route	Treatment Duration
IM EBOV 1000 pfu	1	6 (3M/3F)	Vehicle	Oral	0 mg/kg BID Day 0 0 mg/kg BID Day 1 to Day 13
	2	6 (3M/3F)	T-705	Oral	250 mg/kg twice Day 0 150 mg/kg twice daily BID Day 1 to Day 13
IM MARV 1000 pfu	1	4 (2M/F)	Vehicle	IV	0 mg/kg BID Day 0 0 mg/kg BID Day 1 to Day 13
	2	6 (2M/4F)	T-705	IV	250 mg/kg twice Day 0 150 mg/kg twice daily BID Day 1 to Day 13

3. Results

3.1. T-705 delays time to death in EBOV infected macaques and increases survivorship in MARV infected macaques

Two independent studies were conducted to evaluate the efficacy of T-705 to treat EBOV-Kik or MARV-Ang infected NHPs (Table 1) (Bixler et al., 2017). In each study, cynomolgus macaques were challenged intramuscularly with EBOV-Kik or MARV-Ang on day 0. Macaques infected with EBOV-Kik were orally administered 250 mg kg^{-1} T-705 twice daily on day 0, followed by a 12-day regimen of 150 mg kg^{-1} T-705 twice daily. Another group received vehicle treatment only. Macaques in both treatment groups succumbed to infection, but those treated with T-705 experienced a delayed time to death; median time to death was 7 days post infection for vehicle treated macaques and 15 days for T-705 treated macaques (Fig. 1A, p = 0.0008, Log-rank Mantel-Cox test). Macaques infected with MARV-Ang were intravenously administered vehicle (as experimental control) or 250 mg kg^{-1} T-705 twice daily on day 0, followed by a 12-day regimen of 150 mg kg^{-1} T-705 twice daily. All vehicle-treated animals succumbed as expected. Five of six T-705 treated animals survived, with an extension in the time to death noted in the nonsurvivor. Survival differences were statistically significant (p = 0.0013, Log-rank Mantel-Cox test).

3.2. T-705 reduces viremia in EBOV and MARV infected macaques

The antiviral activity of T-705 on EBOV-Kik or MARV-Ang viral populations *in vivo* was measured by quantifying viral RNA copies and viral titers in day 7 EBOV-Kik and day 6 MARV-Ang plasma samples, when peak viral titers in untreated macaques were reached before succumbing to the infection (Fig. 1B and C) (Bixler et al., 2017). T-705 substantially reduced EBOV-Kik viral RNA copies and viral titers, since many values were below the limits of quantitation (p = < 0.0001, unpaired two-tailed *t*-test). T-705 similarly reduced the viral RNA copies in Day 6 MARV-Ang samples (p = 0.0002, unpaired two-tailed *t*-test). Unfortunately, serum samples were not available for determination of infectious virus in the MARV-Ang NHP experiments, thus specific infectivity could not be calculated.

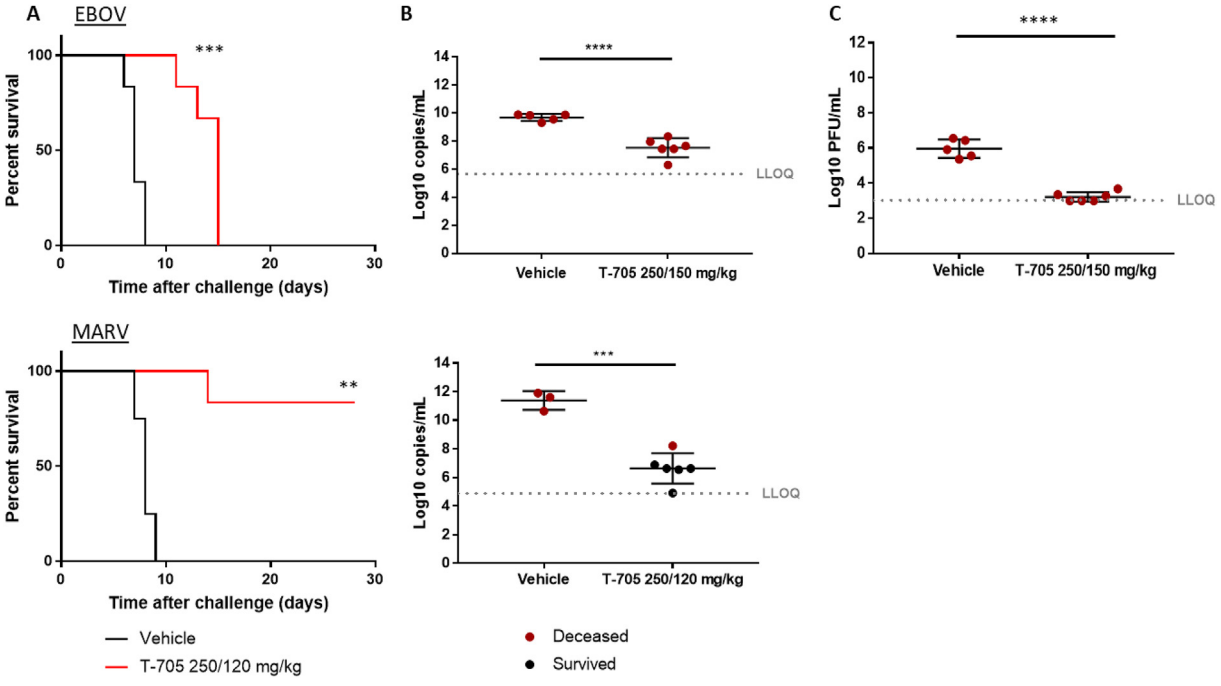

Fig. 1. T-705 increases time to death or survivorship in response to lethal filovirus challenge and exerts antiviral activity in plasma. **a,** Kaplan-Meier survival curves. *P < 0.05 **P < 0.005 ***P < 0.0005 for treatment versus vehicle groups assessed by long-rank (Mantel-Cox) analysis. **b,** Total RNA was extracted from plasma samples from infected macaques and inactivated with 3:1 Trizol LS. Viral genome copies in plasma samples were assessed by qRT-PCR using primers specific to the glycoprotein. Lower limits of quantitation (LLOQ) equal log_{10} 4.9 copies/mL, lower limits of detection (LLOD) is C_t 38.07, approximately log_{10} 3 copies/mL. **c,** Infectious EBOV-Kik viral yields in plasma samples were assessed by plaque assay. Plasma samples from each animal was diluted 10-fold and used to inoculate Vero cells. Plaque forming units (PFU) were quantified 7 days post infection. Treatment groups were compared in an unpaired student T-test, *P < 0.05 **P < 0.005 ***P < 0.0005. LLOQ: Log10 3 PFU/mL. Top, EBOV. Bottom, MARV-Ang.

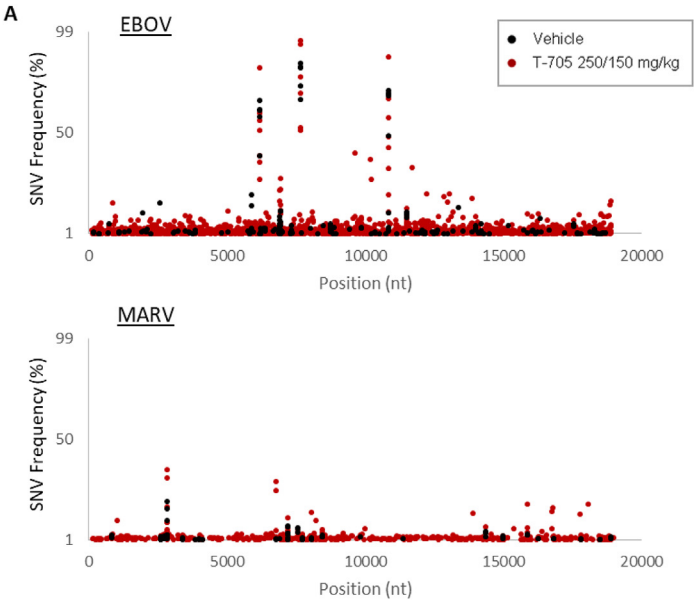

B

Mutation/site/genome	EBOV/Vehicle	SD	EBOV/T-705	SD	P-value
Subclonal Diversity	7.40E-05	1.14E-05	3.65E-04	1.78E-04	0.0056
Transitions	1.94E-05	0	2.72E-04	4.08E-06	0.0207
Transversions	1.62E-05	1.78E-05	3.50E-05	1.99E-04	ns
Indels	2.00E-05	1.27E-05	2.83E-05	1.87E-05	0.0014

Mutation/site/genome	MARV/Vehicle	SD	MARV/T-705	SD	P-value
Subclonal Diversity	2.00E-05	0	6.80E-05	3.35E-05	ns
Transitions	9.00E-06	1.73E-06	8.80E-06	1.64E-06	ns
Transversions	1.67E-05	5.77E-06	6.20E-05	3.63E-05	ns
Indels	5.33E-06	3.06E-06	1.02E-05	5.81E-06	ns

Fig. 2. T-705 increases mutation frequencies in viral populations. **a,** EBOV-Kik or MARV-Ang genomes in plasma samples collected from infected macaques in each study were deep-sequenced using TruSeq RNA Access library preparation and on an Illumina HiSeq or MiSeq platform. Percent intrahost SNV frequency (y axis) across the EBOV genome (x axis) displays increased viral sequence diversity. **b,** The subclonal diversity and the frequency of transitions, transversions, and indels per site per genome were measured for each plasma sample and averaged across treatment groups. Top, EBOV. Bottom, MARV.

3.3. T-705 treatment is associated with increased diversity in EBOV viral populations due to the increase of minority variants

We next sought to identify if T-705 treatment induced lethal mutagenesis in EBOV and MARV populations in these samples.

To identify if T-705 induces mutagenesis of viral genomes, we deep sequenced the EBOV-Kik and MARV-Ang genomes isolated from plasma samples obtained on day 7 and day 6, respectively, and quantified the SNVs in each viral population (Fig. 2A). We obtained 11 EBOV-Kik (5 vehicle, 6 T-705 treated) and 8 MARV-Ang (3 Vehicle, 5 T-705 treated) genomes with sufficient read count (> 500 k reads), depth (> 200 reads per position), and sequence coverage (> 85% viral genome). Analysis of EBOV-Kik and MARV-Ang genomes demonstrates intrahost viral sequence variation in vehicle treated plasma samples. Consensus changes (SNVs > 50%) at positions 6179, 6922, 7668 and 10832 of the EBOV-Kik genomes reflect the diversity of the viral population in the challenge stock (Kugelman et al., 2012). However, we also observe an additional accumulation of low frequency mutations (between 2 and 50% SNV frequency) in T-705 treated macaques as compared to those in untreated macaques. This accumulation is more significant for EBOV-Kik than for MARV-Ang.

Preferential G-to-A and C-to-T changes have been observed in influenza genomes treated with T-705, suggesting that this mutagenic footprint is characteristic of this guanosine analogue (Vanderlinden et al., 2016). The types of base changes in each sample in our study were therefore classified to determine if T-705 treatment displayed a similar activity (Fig. 2B, Supplementary Fig. 1). T-705 induced a significant increase in subclonal diversity in EBOV-Kik genomes with a pattern that could primarily be attributed to a significant increase in the frequency of G-to-A and C-to-T transition mutations ($p = 0.0195$ and 0.0281, respectively, unpaired *t*-test). This pattern of transitions did not show a preferential accumulation for any viral gene (Supplementary Fig. 2). Although subclonal diversity and G-to-A transitions increased in the MARV-Ang viral population of T-705 treated NHPs, the values were not statistically significant. Transitions in the MARV-Ang viral population in T-705 treated NHPs were statistically higher than in vehicle treated NHPs when normalized by read count (Supplementary Fig. 1A). There was no significant difference in indels within or outside of homopolymers (> 4 nucleotides) in filoviral genomes between treatment groups (data not shown).

We measured the correlation between mutagenesis and antiviral activity by comparing the frequency of minor variants with viral titers (Fig. 3) (Guedj et al., 2018). Minor variants are here defined as positions in the viral genome for which the SNV frequency is between 2 and 10%. A nonlinear fit of the data displayed an inverse relationship between EBOV-Kik viral titers or genome copies and the percentage of minor variants in EBOV-Kik genomes ($R^2 = 0.7329$ and 0.8452, respectively). This observation suggests a relationship between low frequency sequence variation and the anti-EBOV activity induced by T-705. While there was little correlation between viral titer and mutagenesis for MARV-Ang genomes ($R^2 = 0.065$), T-705 treated MARV-Ang populations had a lower viral titer and a broader range of minor variants as compared to vehicle treated MARV-Ang populations.

Lethal mutagenesis is also characterized by a reduced infectivity in NA-treated viral populations as compared to non-treated viral populations. Specific infectivity is the ratio of viral particles that can productively infect cells (as measured by viral titers) to the total number of viral particles present (as measured by viral RNA genome copies) (Baranovich et al., 2013; Crotty et al., 2001). The specific infectivity of T-705 treated Ebola viral populations is significantly reduced as compared to vehicle treated populations ($p = < 0.0001$, unpaired two-tailed *t*-test) (Fig. 4). In effect, the total fraction of EBOV-Kik viral population that could initiate a productive infection reduced from ~62% in vehicle treated macaques to ~43% T-705 treated macaques. To control for the specificity of the effect, we also measured the specific infectivity of EBOV-Kik plasma samples taken from the *in vivo* evaluation of an antiviral therapeutic compound with a completely different MOA (e.g., an antisense phosphorodiamidate morpholino oligomer; no possible lethal mutagenesis activity) (Warren et al., 2015). We saw no difference in specific infectivity (data not shown) demonstrating that the changes observed with T-705 are solely related with specific infectivity changes.

3.4. Measuring sequence depth EBOV genomes to indicate chain termination

T-705 has previously demonstrated chain termination activity in EBOV *in vitro* (Jin et al., 2013). T-705 requires two incorporation events for chain termination to occur. We attempted to identify chain

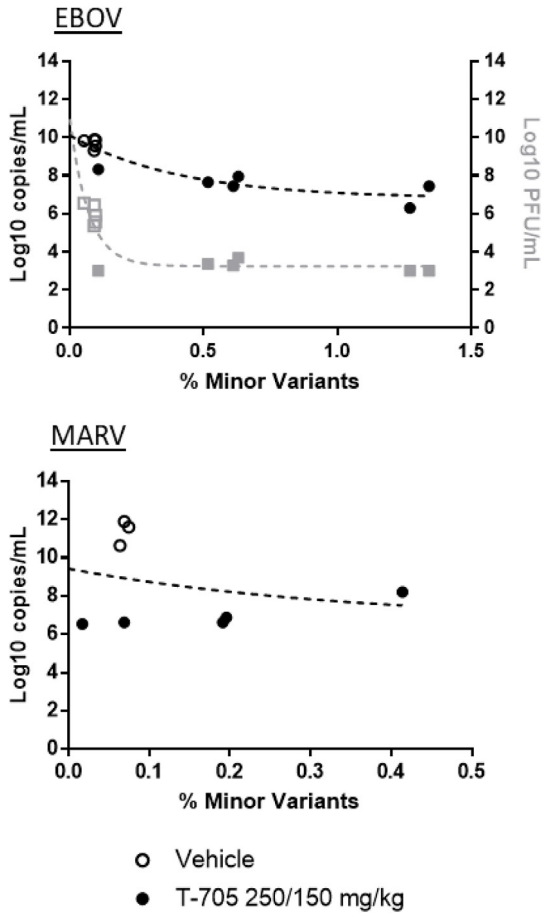

Fig. 3. T-705 decreases viral titers and increases minor variants. The fraction of positions in the viral genome for which SNVs were between 2 and 10% frequency were deemed minor variants. Minor variants measured per day 7 post infection plasma samples (y axis) trended with plaque forming units or viral genome copies. Samples were omitted if viral titer values were unavailable. The best fit nonlinear one phase decay regression line was applied to values across treatment groups. Log10 GE/mL v % minor variants (EBOV): $R^2 = 0.8452$. Log10 Plaque v % minor variants (EBOV): $R^2 = 0.7329$. Log10 GE/mL v % minor variants (MARV): $R^2 = 0.065$.

termination in the available EBOV-Kik and MARV-Ang genomic data by measuring a change in the viral transcriptional gradient (Shabman et al., 2014). To do so, we measured the average sequence depth in positively and negatively stranded viral RNA across the genome for each sample (Fig. 5). Although these samples were derived from plasma for which the majority of the viral RNA is expected to be full length negative stranded genomes in virions, a smaller fraction of the RNA will be positive stranded viral mRNA produced in the context of NA treatment (Whitmer et al., 2018) (Supplementary Fig. 3). In vehicle-treated samples, we observe an equal depth across the negative-stranded RNA genome, in which full length RNA genomes are packaged into virions, and the natural decrease of positive-stranded viral mRNAs along the viral genome reflecting the EBOV-Kik transcriptional gradient, in which viral NP mRNA is generated at higher quantities than L mRNA (Shabman et al., 2014). Sequences from T-705 treated macaques show no differences in sequence depth across the negative stranded EBOV-Kik genomes and a shallower positive stranded transcriptional gradient in the NP gene as compared to vehicle, suggesting an impact on viral mRNA. The transcriptional gradient of T-705 treated MARV-Ang positive strand RNA is similarly altered. Deep sequencing of tissue samples at sites of active viral replication could further clarify the effect of T-705 on the generation of filoviral genomes and transcripts.

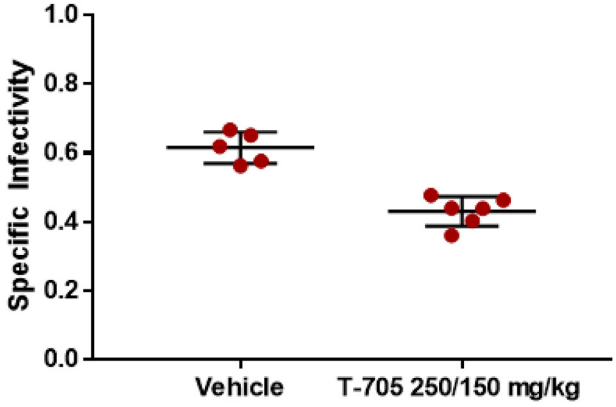

Fig. 4. T-705 reduces the specific infectivity of EBOV-Kik populations in macaque plasma at day 7 post infection. Specific infectivity values were calculated as the ratio of infectious viral yield to total virus genome copies. The ratio of the log10 PFU/mL to log10 copies/mL from each macaque at day 7 post infection was calculated. Values < LOQ in plaque assays were set at log10 3 PFU/mL. Values between the LLOQ and LOD in qRT-PCR assays were set at log10 4.9 copies/mL. Treatment groups were compared in an unpaired student T-test, *P < 0.05 **P < 0.005 ***P < 0.0005. Samples were labeled if they derived from macaques that deceased (red) or survived (black) the study.

4. Discussion

Nucleoside analogues that exhibit antiviral activity against RNA viruses are one of many classes of compounds evaluated for its capacity to treat lethal EBOV infection (Cross et al., 2018). The failure of the JIKI trial called into question the use of T-705 as a therapeutic for EBOV infections (Nguyen et al., 2017; Sissoko et al., 2016). Two animal studies designed to test the efficacy of T-705 against a lethal challenge of EBOV and MARV provided an opportunity to identify the *in vivo* mechanisms of therapeutic activity of this compound (Bixler et al., 2017). Here, we add deep sequencing to the clinical and virologic analysis of these studies to demonstrate that the MOA that T-705 uses to exert antiviral activity against EBOV and MARV *in vivo* may be attributed to lethal mutagenesis.

We first observed that T-705 increased mutagenesis was associated with antiviral activity *in vivo* in Ebola populations. The result of this was a decrease in specific infectivity, which is characteristic of lethal mutagenesis. Specific infectivity reflects the reduced infectious and replicative capacity of viral populations (Crotty and Andino, 2002; Crotty et al., 2001). We observed that the specific infectivity of vehicle and T-705 treated EBOV populations were ~0.62 and ~0.43 log10 PFU/mL/log10 RNA copies/mL, respectively, indicating that T-705 treatment impairs viral replication efficiency. While this value is not a precise measurement of true infectivity in the viral population, as plaque assay and qRT-PCR values reached the limits of quantitation in our assays, we can assume that these values are overestimations and that T-705 has a more significant deleterious effect on viral replication.

We also suggest a method to detect chain termination could be detected in *in vivo* EBOV and MARV populations by measuring changes in the transcriptional gradient of from deep sequencing read depths. Previously, this MOA could only be demonstrated by incubating RdRP with T-705 and measuring inhibition of RNA elongation, *in vitro*. Our study opens the possibility of "quantifying" the contribution of each MOA to the antiviral activity of nucleoside analogues. Chain termination should inhibit the production of full-length mRNA transcripts, genomes, or antigenomes. Thus, stranded read depth along the genome could be used to identify changes in genome sequence coverage for each type of viral nucleic acids. Using sequencing methods that allow us to perform such evaluation, we saw no change in relative coverage of negative strand viral genomes and a flattening of the positive strand transcriptional gradient in T-705 treated viral populations. Deep

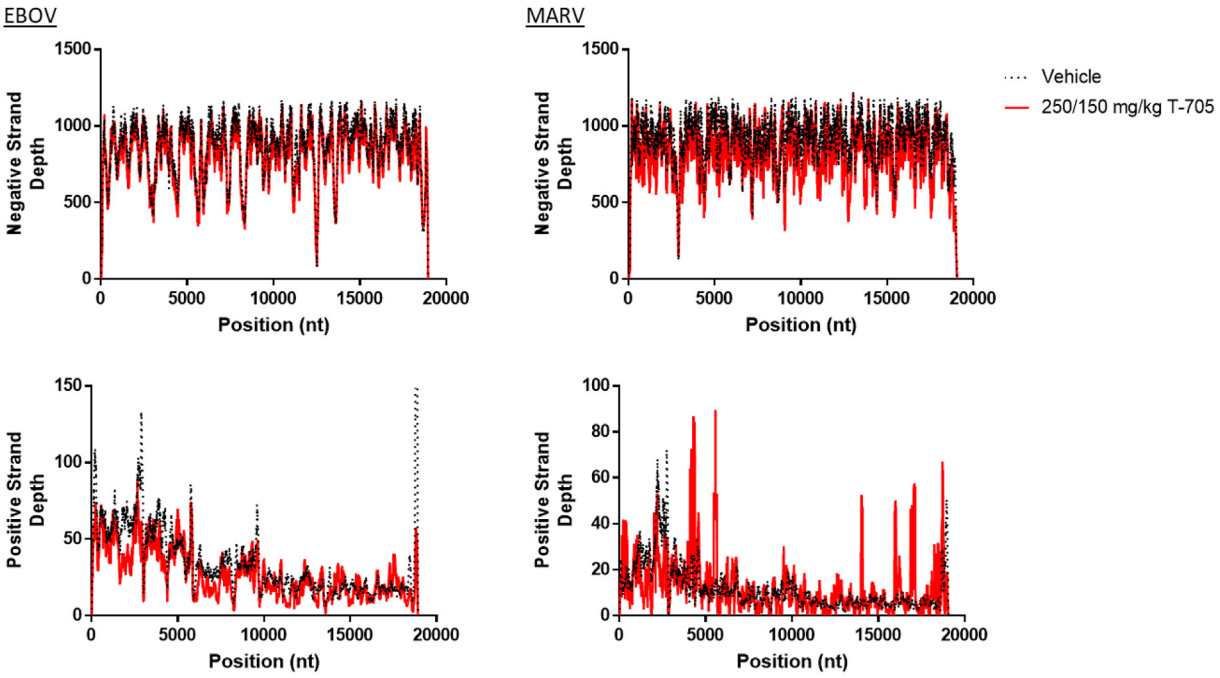

Fig. 5. Sequence depth of stranded viral genomes in plasma samples changes with T-705 treatment. Binary alignment files containing viral reads (read 1 only) from day 7 plasma samples were segregated by positive or negative strandedness. The average sequence depth (y axis) was mapped across the viral genome (x axis). Left, EBOV. Right, MARV. MARV-Ang sample 9869 was excluded for low depth of positive stranded reads.

sequencing of viral populations in tissues from treated NHPs should be evaluated to determine if chain termination is occurring during genome replication.

Guedj and collegues conducted a similar study in which 2 of 5 cynomolgus macaques survived a 1000 pfu challenge of Ebola virus Gabon 2001 strain when treated with a 13-day course of 250/150 mg/kg T-705 (Guedj et al., 2018). Increased mutagenesis was also associated with antiviral activity in that study. Our data confirmed Guedj's findings and expanded those results by demonstrating that the associated increased mutagenesis was also observed in MARV- treated NHPs. Based on available data we cannot determine the reason behind the greater survival of EBOV-infected NHPs observed in Guedj et al. studies in comparison with the delayed time to death in our EBOV studies, it is possible that T-705 antiviral activity differs between virus variants as that is the only apparent difference between both experimental designs. If true, it would be imperative that the development of T-705, or other NAs, for therapeutic use against filoviruses be assessed for antiviral activity against divergent viral strains early in development.

In this study, we characterized the antiviral activity of T-705 against filoviral infections in NHPs and attributed the apparent MOA to lethal mutagenesis. This study also demonstrated that an *in vivo* MOA can be characterized by conducting common genomic analyses using ex vivo (and potentially clinical) samples. Future attempts to develop NAs for therapeutic use in humans should employ genomic analyses to further characterize the MOA of NAs and assess its use as an indicator of drug activity.

Disclaimer

Opinions, interpretations, conclusions, and recommendations are those of the authors and are not necessarily endorsed by the US Army.

Funding

This work was supported by the Joint Science and Technology Office for Chemical and Biological Defense, Defense Threat Reduction Agency (plan CB10246) and MCS.

Transparency declarations

All authors: No reported conflicts of interest.

Acknowledgements

We thank Dr. Eric Donaldson of the US Food and Drug Administration for his expertise in experimental design for the NHP studies and commentary during manuscript preparation.

Appendix A. Supplementary data

Supplementary data to this article can be found online at https://doi.org/10.1016/j.antiviral.2019.06.001.

References

Andino, R., Domingo, E., 2015. Viral quasispecies. Virology 479–480, 46–51.
Arias, A., Thorne, L., Goodfellow, I., 2014. Favipiravir elicits antiviral mutagenesis during virus replication in vivo. Elife 3, e03679.
Arts, E.J., Wainberg, M.A., 1994. Preferential incorporation of nucleoside analogs after template switching during human immunodeficiency virus reverse transcription. Antimicrob. Agents Chemother. 38, 1008–1016.
Arts, E.J., Wainberg, M.A., 1996. Mechanisms of nucleoside analog antiviral activity and resistance during human immunodeficiency virus reverse transcription. Antimicrob. Agents Chemother. 40, 527–540.
Asahina, Y., Izumi, N., Enomoto, N., Uchihara, M., Kurosaki, M., Onuki, Y., Nishimura, Y., Ueda, K., Tsuchiya, K., Nakanishi, H., Kitamura, T., Miyake, S., 2005. Mutagenic effects of ribavirin and response to interferon/ribavirin combination therapy in chronic hepatitis C. J. Hepatol. 43, 623–629.
Baranovich, T., Wong, S.S., Armstrong, J., Marjuki, H., Webby, R.J., Webster, R.G., Govorkova, E.A., 2013. T-705 (favipiravir) induces lethal mutagenesis in influenza A H1N1 viruses in vitro. J. Virol. 87, 3741–3751.
Bixler, S.L., Bocan, T.M., Wells, J., Wetzel, K., Van Tongeren, S., Dong, L., Lackemeyer, N., Donnelly, G., Cazares, L., Nuss, J., Soloveva, V., Koistinen, K., Welch, L., Epstein, C., Liang, L.F., Giesing, D., Lenk, R., Bavari, S., Warren, T.K., 2017. Efficacy of favipiravir (T-705) in nonhuman primates infected with Ebola virus or Marburg virus. Antivir. Res. 151, 97–104.
Borodina, T., Adjaye, J., Sultan, M., 2011. A strand-specific library preparation protocol for RNA sequencing. Methods Enzymol. 500, 79–98.

Cross, R.W., Mire, C.E., Feldmann, H., Geisbert, T.W., 2018. Post-exposure treatments for Ebola and Marburg virus infections. Nat. Rev. Drug Discov. 17, 413–434.
Crotty, S., Andino, R., 2002. Implications of high RNA virus mutation rates: lethal mutagenesis and the antiviral drug ribavirin. Microb. Infect. 4, 1301–1307.
Crotty, S., Cameron, C.E., Andino, R., 2001. RNA virus error catastrophe: direct molecular test by using ribavirin. Proc. Natl. Acad. Sci. U. S. A. 98, 6895–6900.
de Avila, A.I., Gallego, I., Soria, M.E., Gregori, J., Quer, J., Esteban, J.I., Rice, C.M., Domingo, E., Perales, C., 2016. Lethal mutagenesis of hepatitis C virus induced by favipiravir. PLoS One 11, e0164691.
Delang, L., Segura Guerrero, N., Tas, A., Querat, G., Pastorino, B., Froeyen, M., Dallmeier, K., Jochmans, D., Herdewijn, P., Bello, F., Snijder, E.J., de Lamballerie, X., Martina, B., Neyts, J., van Hemert, M.J., Leyssen, P., 2014. Mutations in the chikungunya virus non-structural proteins cause resistance to favipiravir (T-705), a broad-spectrum antiviral. J. Antimicrob. Chemother. 69, 2770–2784.
Dietz, J., Schelhorn, S.E., Fitting, D., Mihm, U., Susser, S., Welker, M.W., Fuller, C., Daumer, M., Teuber, G., Wedemeyer, H., Berg, T., Lengauer, T., Zeuzem, S., Herrmann, E., Sarrazin, C., 2013. Deep sequencing reveals mutagenic effects of ribavirin during monotherapy of hepatitis C virus genotype 1-infected patients. J. Virol. 87, 6172–6181.
Drake, J.W., Holland, J.J., 1999. Mutation rates among RNA viruses. Proc. Natl. Acad. Sci. U. S. A. 96, 13910–13913.
Espy, N., Perez-Sautu, U., Ramirez de Arellano, E., Negredo, A., Wiley, M.R., Bavari, S., Diaz Menendez, M., Sanchez-Seco, M.P., Palacios, G., 2018. Ribavirin had demonstrable effects on the crimean-Congo hemorrhagic fever virus (CCHFV) population and load in a patient with CCHF infection. J. Infect. Dis. 217, 1952–1956.
Fung, A., Jin, Z., Dyatkina, N., Wang, G., Beigelman, L., Deval, J., 2014. Efficiency of incorporation and chain termination determines the inhibition potency of 2'-modified nucleotide analogs against hepatitis C virus polymerase. Antimicrob. Agents Chemother. 58, 3636–3645.
Guedj, J., Piorkowski, G., Jacquot, F., Madelain, V., Nguyen, T.H.T., Rodallec, A., Gunther, S., Carbonnelle, C., Mentre, F., Raoul, H., de Lamballerie, X., 2018. Antiviral efficacy of favipiravir against Ebola virus: a translational study in cynomolgus macaques. PLoS Med. 15, e1002535.
Guide for the Care and Use of Laboratory Animals.
Jin, Z., Smith, L.K., Rajwanshi, V.K., Kim, B., Deval, J., 2013. The ambiguous base-pairing and high substrate efficiency of T-705 (Favipiravir) Ribofuranosyl 5'-triphosphate towards influenza A virus polymerase. PLoS One 8, e68347.
Kugelman, J.R., Lee, M.S., Rossi, C.A., McCarthy, S.E., Radoshitzky, S.R., Dye, J.M., Hensley, L.E., Honko, A., Kuhn, J.H., Jahrling, P.B., Warren, T.K., Whitehouse, C.A., Bavari, S., Palacios, G., 2012. Ebola virus genome plasticity as a marker of its passaging history: a comparison of in vitro passaging to non-human primate infection. PLoS One 7, e50316.
Kugelman, Jeffrey R., Kugelman-Tonos, J., Ladner, Jason T., Pettit, J., Keeton, Carolyn M., Nagle, Elyse R., Garcia, Karla Y., Froude, Jeffrey W., Kuehne, Ana I., Kuhn, Jens H., Bavari, S., Zeitlin, L., Dye, John M., Olinger, Gene G., Sanchez-Lockhart, M., Palacios, Gustavo F., 2015a. Emergence of ebola virus escape variants in infected nonhuman primates treated with the MB-003 antibody cocktail. Cell Rep. 12, 2111–2120.
Kugelman, J.R., Wiley, M.R., Mate, S., Ladner, J.T., Beitzel, B., Fakoli, L., Taweh, F., Prieto, K., Diclaro, J.W., Minogue, T., Schoepp, R.J., Schaecher, K.E., Pettitt, J., Bateman, S., Fair, J., Kuhn, J.H., Hensley, L., Park, D.J., Sabeti, P.C., Sanchez-Lockhart, M., Bolay, F.K., Palacios, G., 2015b. US Army Medical Research Institute of Infectious Diseases; National Institutes of Health; Integrated Research Facility - Frederick Ebola Response Team 2014-2015, Monitoring of ebola virus makona evolution through establishment of advanced genomic capability in Liberia. Emerg. Infect. Dis. 21, 1135–1143.
Kugelman, J.R., Rossi, C.A., Wiley, M.R., Ladner, J.T., Nagle, E.R., Pfeffer, B.P., Garcia, K., Prieto, K., Wada, J., Kuhn, J.H., Palacios, G., 2016. Informing the historical record of experimental nonhuman primate infections with ebola virus: genomic characterization of USAMRIID ebola virus/H.sapiens-tc/COD/1995/Kikwit-9510621 challenge stock "R4368" and its replacement "R4415". PLoS One 11, e0150919.
Kugelman, J.R., Wiley, M.R., Nagle, E.R., Reyes, D., Pfeffer, B.P., Kuhn, J.H., Sanchez-Lockhart, M., Palacios, G.F., 2017. Error baseline rates of five sample preparation methods used to characterize RNA virus populations. PLoS One 12, e0171333.
Kuhn, J.H., 2008. Filoviruses. A compendium of 40 years of epidemiological, clinical, and laboratory studies. Archives of virology. Supplement 20 13-360.
Lee, W.P., Stromberg, M.P., Ward, A., Stewart, C., Garrison, E.P., Marth, G.T., 2014. MOSAIK: a hash-based algorithm for accurate next-generation sequencing short-read mapping. PLoS One 9, e90581.
Li, H., Handsaker, B., Wysoker, A., Fennell, T., Ruan, J., Homer, N., Marth, G., Abecasis, G., Durbin, R., 2009. The sequence alignment/map format and SAMtools. Bioinformatics 25, 2078–2079.
Nguyen, T.H., Guedj, J., Anglaret, X., Laouenan, C., Madelain, V., Taburet, A.M., Baize, S., Sissoko, D., Pastorino, B., Rodallec, A., Piorkowski, G., Carazo, S., Conde, M.N., Gala, J.L., Bore, J.A., Carbonnelle, C., Jacquot, F., Raoul, H., Malvy, D., de Lamballerie, X., Mentre, F., group, J.s., 2017. Favipiravir pharmacokinetics in Ebola-Infected patients of the JIKI trial reveals concentrations lower than targeted. PLoS Neglected Trop. Dis. 11, e0005389.
Oestereich, L., Ludtke, A., Wurr, S., Rieger, T., Munoz-Fontela, C., Gunther, S., 2014. Successful treatment of advanced Ebola virus infection with T-705 (favipiravir) in a small animal model. Antivir. Res. 105, 17–21.
Sanchez, A., Kiley, M.P., Holloway, B.P., Auperin, D.D., 1993. Sequence analysis of the Ebola virus genome: organization, genetic elements, and comparison with the genome of Marburg virus. Virus Res. 29, 215–240.
Sanjuan, R., Nebot, M.R., Chirico, N., Mansky, L.M., Belshaw, R., 2010. Viral mutation rates. J. Virol. 84, 9733–9748.
Shabman, R.S., Jabado, O.J., Mire, C.E., Stockwell, T.B., Edwards, M., Mahajan, M., Geisbert, T.W., Basler, C.F., 2014. Deep sequencing identifies noncanonical editing of Ebola and Marburg virus RNAs in infected cells. mBio 5, e02011.
Sissoko, D., Laouenan, C., Folkesson, E., M'Lebing, A.B., Beavogui, A.H., Baize, S., Camara, A.M., Maes, P., Shepherd, S., Danel, C., Carazo, S., Conde, M.N., Gala, J.L., Colin, G., Savini, H., Bore, J.A., Le Marcis, F., Koundouno, F.R., Petitjean, F., Lamah, M.C., Diederich, S., Tounkara, A., Poelart, G., Berbain, E., Dindart, J.M., Duraffour, S., Lefevre, A., Leno, T., Peyrouset, O., Irenge, L., Bangoura, N., Palich, R., Hinzmann, J., Kraus, A., Barry, T.S., Berette, S., Bongono, A., Camara, M.S., Munoz, V.C., Doumbouya, L., Harouna, S., Kighoma, P.M., Koundouno, F.R., Lolamou, R., Loua, C.M., Massala, V., Moumouni, K., Provost, C., Samake, N., Sekou, C., Soumah, A., Arnould, I., Komano, M.S., Gustin, L., Berutto, C., Camara, D., Camara, F.S., Colpaert, J., Delamou, L., Jansson, L., Kourouma, E., Loua, M., Malme, K., Manfrin, E., Maomou, A., Milinouno, A., Ombelet, S., Sidiboun, A.Y., Verreckt, I., Yombouno, P., Bocquin, A., Carbonnelle, C., Carmoi, T., Frange, P., Mely, S., Nguyen, V.K., Pannetier, D., Taburet, A.M., Treluyer, J.M., Kolie, J., Moh, R., Gonzalez, M.C., Kuisma, E., Liedigk, B., Ngabo, D., Rudolf, M., Thom, R., Kerber, R., Gabriel, M., Di Caro, A., Wolfel, R., Badir, J., Bentahir, M., Deccache, Y., Dumont, C., Durant, J.F., El Bakkouri, K., Uwamahoro, M.G., Smits, B., Toufik, N., Van Cauwenberghe, S., Ezzedine, K., D'Ortenzio, E., Pizarro, L., Etienne, A., Guedj, J., Fizet, A., de Sainte Fare, E.B., Murgue, B., Tran-Minh, T., Rapp, C., Piguet, P., Poncin, M., Draguez, B., Duverger, T.A., Barbe, S., Baret, G., Defourny, I., Carroll, M., Raoul, H., Augier, A., Eholie, S.P., Yazdanpanah, Y., Levy-Marchal, C., Antierrens, A., Van Herp, M., Gunther, S., de Lamballerie, X., Keita, S., Mentre, F., Anglaret, X., Malvy, D., Group, J.S., 2016. Correction: experimental treatment with favipiravir for ebola virus disease (the JIKI trial): a historically controlled, single-arm proof-of-concept trial in Guinea. PLoS Med. 13, e1002009.
Smither, S.J., Eastaugh, L.S., Steward, J.A., Nelson, M., Lenk, R.P., Lever, M.S., 2014. Post-exposure efficacy of oral T-705 (Favipiravir) against inhalational Ebola virus infection in a mouse model. Antivir. Res. 104, 153–155.
Vanderlinden, E., Vrancken, B., Van Houdt, J., Rajwanshi, V.K., Gillemot, S., Andrei, G., Lemey, P., Naesens, L., 2016. Distinct effects of T-705 (favipiravir) and ribavirin on influenza virus replication and viral RNA synthesis. Antimicrob. Agents Chemother. 60, 6679–6691.
Warren, T.K., Whitehouse, C.A., Wells, J., Welch, L., Heald, A.E., Charleston, J.S., Sazani, P., Reid, S.P., Iversen, P.L., Bavari, S., 2015. A single phosphorodiamidate morpholino oligomer targeting VP24 protects rhesus monkeys against lethal Ebola virus infection. mBio 6.
Warren, T.K., Jordan, R., Lo, M.K., Ray, A.S., Mackman, R.L., Soloveva, V., Siegel, D., Perron, M., Bannister, R., Hui, H.C., Larson, N., Strickley, R., Wells, J., Stuthman, K.S., Van Tongeren, S.A., Garza, N.L., Donnelly, G., Shurtleff, A.C., Retterer, C.J., Gharaibeh, D., Zamani, R., Kenny, T., Eaton, B.P., Grimes, E., Welch, L.S., Gomba, L., Wilhelmsen, C.L., Nichols, D.K., Nuss, J.E., Nagle, E.R., Kugelman, J.R., Palacios, G., Doerffler, E., Neville, S., Carra, E., Clarke, M.O., Zhang, L., Lew, W., Ross, B., Wang, Q., Chun, K., Wolfe, L., Babusis, D., Park, Y., Stray, K.M., Trancheva, I., Feng, J.Y., Barauskas, O., Xu, Y., Wong, P., Braun, M.R., Flint, M., McMullan, L.K., Chen, S.S., Fearns, R., Swaminathan, S., Mayers, D.L., Spiropoulou, C.F., Lee, W.A., Nichol, S.T., Cihlar, T., Bavari, S., 2016. Therapeutic efficacy of the small molecule GS-5734 against Ebola virus in rhesus monkeys. Nature 531, 381–385.
Whitmer, S.L.M., Ladner, J.T., Wiley, M.R., Patel, K., Dudas, G., Rambaut, A., Sahr, F., Prieto, K., Shepard, S.S., Carmody, E., Knust, B., Naidoo, D., Deen, G., Formenty, P., Nichol, S.T., Palacios, G., Stroher, U., 2018. Active ebola virus replication and heterogeneous evolutionary rates in EVD survivors. Cell Rep. 22, 1159–1168.